

Piezo-Phototronic Effect Modulated Deep UV Photodetector Based on ZnO-Ga₂O₃ Heterojunction Microwire

Mengxiao Chen, Bin Zhao, Guofeng Hu, Xiaosheng Fang,* Hui Wang,* Lei Wang, Jun Luo, Xun Han, Xiandi Wang, Caofeng Pan,* and Zhong Lin Wang*

A strain modulated solar-blinded photodetector (PD) based on ZnO-Ga₂O₃ core-shell heterojunction microwire is developed. This PD is highly sensitive to deep UV light centered at 261 nm. It performs ultrahigh sensitivity and spectral selectivity, which can response to rare weak deep UV light ($\approx 1.3 \mu\text{W cm}^{-2}$) and almost no response to visible light wavelength ranges. Moreover, by using the piezo-phototronic effect, the deep UV current response is enhanced to about three times under -0.042% static strain. This is a three way coupling effect among piezoelectric polarization, semiconductor properties, and optical excitation, which exists in noncentral symmetric wurtzite semiconductors such as ZnO, GaN, and CdS. By modulating the energy band diagrams and charge carriers in the junction area upon straining, the optoelectronic processes are regulated. The strain induced piezopotential modulates carrier transport in the heterostructure, which improves the response of the PD, with potential applications for health monitoring, smart systems, deep space exploration, and security communication.

gap mismatch among materials used in commercial photodetectors (PDs), detections of wavelength in deep UV ranges have not been fully achieved. Light in this wavelength range (wave band) possesses higher energy and a strong penetrability. Thus deep UV detection plays a significant role in our life,^[3] especially in health monitoring, security communication, and deep space exploration. In order to solve this problem, tremendous efforts have been put into the material research^[4] and found that, with a direct wide band gap ($\approx 4.9 \text{ eV}$), $\beta\text{-Ga}_2\text{O}_3$ is quite suitable for solar-blinded photodetection.^[5] When it comes to specific device design, the photovoltaic detector is a preferred choice for its fast response and well-developed manufacturing technology,^[6] and it is also the foundation of PD structure. As $\beta\text{-Ga}_2\text{O}_3$ performs n-type conductivity,

a heterojunction photovoltaic photodetector based on $\beta\text{-Ga}_2\text{O}_3$ could be a feasible solution.^[7] Moreover, with the coefficient of piezo-phototronic effect,^[8] the detection is expected to be connected with human-machine interaction. By constructing a Ga₂O₃-ZnO heterostructure,^[9] the strain induced piezopotential in ZnO modulates carrier transport in the junction area, which could improve the response of the PD. Piezo-phototronic effect is a three way coupling effect of piezoelectric polarization,

1. Introduction

Photodetectors which are important components in modern optoelectronic systems have been studied for decades.^[1] Photodetectors including photomultiplier, light dependent resistor, and photodiode have been commercially manufactured and widely used in imaging systems and our daily life,^[2] target tracing, spectral analysis, and so on. However, due to the band

M. Chen, Dr. G. Hu, X. Han, Dr. X. Wang, Prof. C. Pan, Prof. Z. L. Wang
CAS Center for Excellence in Nanoscience
Beijing Institute of Nanoenergy and Nanosystems
Chinese Academy of Sciences
Beijing 100083, China
E-mail: cfpan@binn.cas.cn; zhong.wang@mse.gatech.edu

M. Chen, Dr. G. Hu, X. Han, Dr. X. Wang, Prof. C. Pan, Prof. Z. L. Wang
School of Nanoscience and Technology
University of Chinese Academy of Sciences
Beijing 100049, P. R. China

Dr. B. Zhao, Prof. X. Fang
Department of Materials Science
Fudan University
Shanghai 200433, P. R. China
E-mail: xshfang@fudan.edu.cn

Prof. H. Wang
Key Laboratory of Aerospace Materials and Performance
(Ministry of Education)
School of Materials Science and Engineering
Beihang University
Beijing 100191, P. R. China
E-mail: huiwang@buaa.edu.cn

Dr. L. Wang, Prof. J. Luo
Center for Electron Microscopy
Tianjin University of Technology
Tianjin 300384, P. R. China

Prof. Z. L. Wang
School of Materials Science and Engineering
Georgia Institute of Technology
Atlanta, GA 30332-0245, USA

 The ORCID identification number(s) for the author(s) of this article can be found under <https://doi.org/10.1002/adfm.201706379>.

DOI: 10.1002/adfm.201706379

semiconductor properties, and optical excitation, which exists in noncentral symmetric wurtzite semiconductors such as ZnO,^[10] GaN,^[11] CdS,^[12] and so on. This effect has been reported to efficiently manipulate the current response of photodetectors,^[13] emission intensity of light-emitting diodes (LEDs),^[14] and the efficiency of solar cells^[15] by utilizing the piezopolarization charges created at the junction upon straining, with optoelectronic processes regulated, such as generation, separation, recombination, and transport of charge carriers.^[8,16]

Here, we developed a strain modulated solar-blinded photo-detector based on ZnO-Ga₂O₃ core-shell heterojunction microwire. ZnO-Ga₂O₃ core-shell microwires were grown through one-step approach with the ZnO core single-crystalline and the Ga₂O₃ shell polycrystalline. This PD is highly sensitive to deep UV light due to the direct wide band gap (≈ 4.9 eV) of Ga₂O₃, the heterostructure, and a large specific surface area of the single microwire. It demonstrated ultrahigh sensitivity, high signal-to-noise ratio, and high spectral selectivity. Moreover, the detection could be enhanced by applying certain static strain on the device through the piezo-phototronic effect. The current response was enhanced to about three times under -0.042% strain. The strain induced piezopotential modulates carrier transport both in the ZnO core and at the junction area. The current response of this PD was enhanced by this effect and thus made it more perspective in health monitoring,^[17] smart systems,^[18] deep space exploration, and security communication.^[19]

2. Results and Discussion

The ZnO-Ga₂O₃ core-shell microwires were grown through one-step chemical vapor deposition (CVD) approach.^[20] Figure 1a shows the structure design of the ZnO core-Ga₂O₃ shell microwire solar-blinded PD, which could be regulated by external strains. The microwire was transferred onto the polyethylene terephthalate (PET) substrate to make it a flexible device. Linear I - V curves of the individual ZnO microwire and the heterostructure microwire with Ag electrodes are shown in Figure S1 in the Supporting Information and indicate the ohmic contacts. First the I - t on-off test was carried out using a commercial mercury lamp to affirm its sensitivity to UV light. The I - t response curve in Figure 1b under $229 \mu\text{W cm}^{-2}$ shows the rise time <0.3 s and recover time <0.3 s (defining the rise and recover time as the time needed to reach 90% of the full response). After confirming the performance to sense the UV light, the specific detecting sensitivity was measured to get the specific wavelength range which this microwire PD most sensitive to. As shown in Figure 1c, this solar-blinded PD is mostly sensitive to light range from 245 to 280 nm centering at 261 nm. The responsivity was gained from the photo-response showed in the inset and the wavelength intensities of the applied light source (Figure S2, Supporting Information). From the inset we could notice that the this PD perform the best current response under 268 nm, so a series of test were carried out under 268 nm UV light. Transmission electron

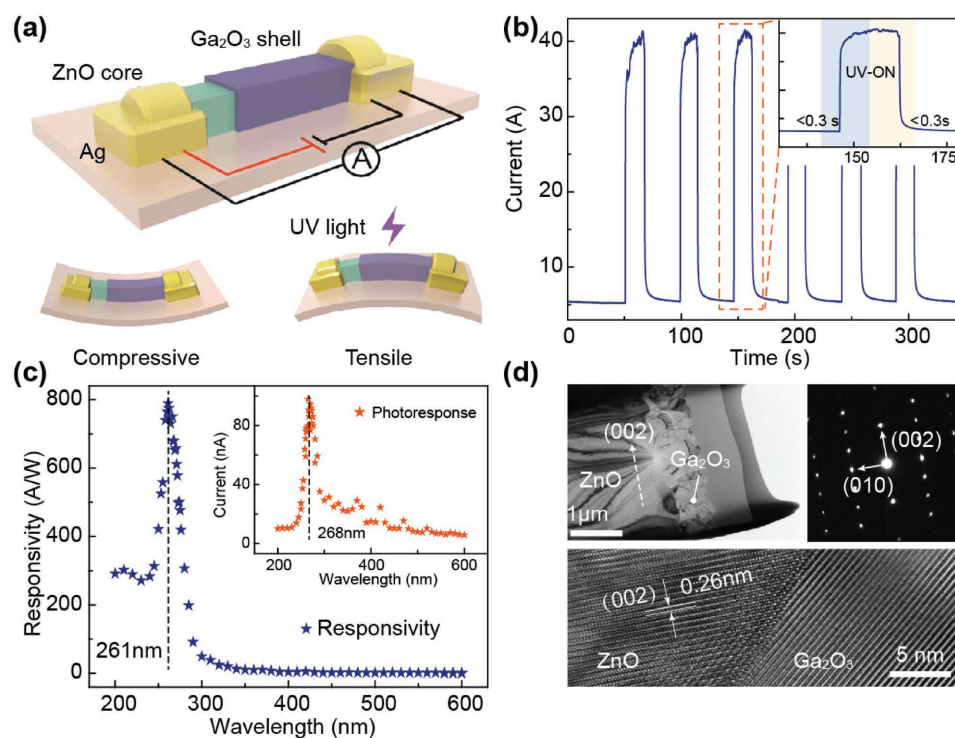


Figure 1. a) Structure design of the ZnO-Ga₂O₃ core-shell microwire PD. b) I - t response curve under $229 \mu\text{W cm}^{-2}$ mercury lamp with rise time <0.3 s and recover time <0.3 s. c) Detecting sensitivity depending on wavelength. This device is most sensitive to 261 nm wavelength according to the responsivity, which was gained by processing the photoresponse data and the light intensities. The inset is the current response under light with different wavelengths. Figure S2 in the Supporting Information shows the wavelength intensity of the light source. d) TEM image of the core-shell structure. The top-left inset is the sample in a lower magnification and the top-right inset is the selected area electron diffraction. The ZnO core is monocrystalline, while the Ga₂O₃ shell is polycrystalline. The c -axis of ZnO core is along the microwire.

microscopy (TEM) results in Figure 1d show the single-crystalline ZnO core and polycrystalline Ga₂O₃ shell, with the *c*-axis of ZnO along the direction of the microwire. The sample used in Figure 1d was fabricated along the microwire, and samples perpendicular to the microwire direction were also made to confirm the *c*-axis of ZnO. Figures S3 and S4 show the TEM results from two microwires and prove the above conclusion and Figure S5 shows the interface of the heterostructure with a high magnification to see the polycrystalline Ga₂O₃ shell.

To systematically investigate the optical properties of this newly developed deep-UV photodetector, a series of measurements were proceeded/adopted. As Figure 2a shows, a rectangular wave stimuli was applied on the device, and then it was exposed to different light source to obtain the responses. The green line is the original curve in the dark environment, the purple line is the response under 56.344 μW cm⁻² natural light illuminating, and the blue line represents response under 1.04 μW cm⁻² 268 nm UV light. The response to 268 nm UV light is much larger than the natural light illuminating though its intensity is extremely weak. The results indicate that this microwire PD is of high spectral selectivity and ultrahigh sensitivity. We further studied the performance to light intensity under specific wavelength. Figure 2b are *I*-*V* responses under different light intensities of 268 nm UV light, which perform a speciality

to identify a rare small change in light intensity (0.03 μW cm⁻²). Figure 2c is the *I*-*t* on-off test of the device with light intensities accord with Figure 2b. The illumination intensity dependence of photocurrents ($I_{ph} = I_{light} - I_{dark}$) was calculated and plotted in Figure 2d. The photocurrents increased upon enhancing the illumination intensity without saturations. The sensitivity defined as I_{ph}/I_{dark} was calculated to be 1101% under 1.994 μW cm⁻² 268 nm UV illumination. Moreover, the photoresponsivity *R*, which is defined as I_{ph}/P_{ill} , where P_{ill} is the illumination power on the PD, is also a critical parameter to evaluate the performances of the deep-UV PD. From Figure 2e, the photoresponsivity increased upon increasing the illumination intensity, with the range 1.7–2.0 μW cm⁻² solar blind illumination.

Sequentially we measured the strain modulated performances for this PD device. In order to introduce strains and light in the same time, a testing platform composed of laser-driven light sources, monochromator, signal generator, electrometer and 3D stages was developed. Through this testing system, we could achieve both optical property measurements (Figure 1c and Figure 2) and mechanical property measurements, both carrying on independent tests and studying the coupling effect simultaneously. By applying a triangular wave across the device swiping from -2 to +2 V, we could visually observe the piezoelectric effect on *I*-*V* curves. When

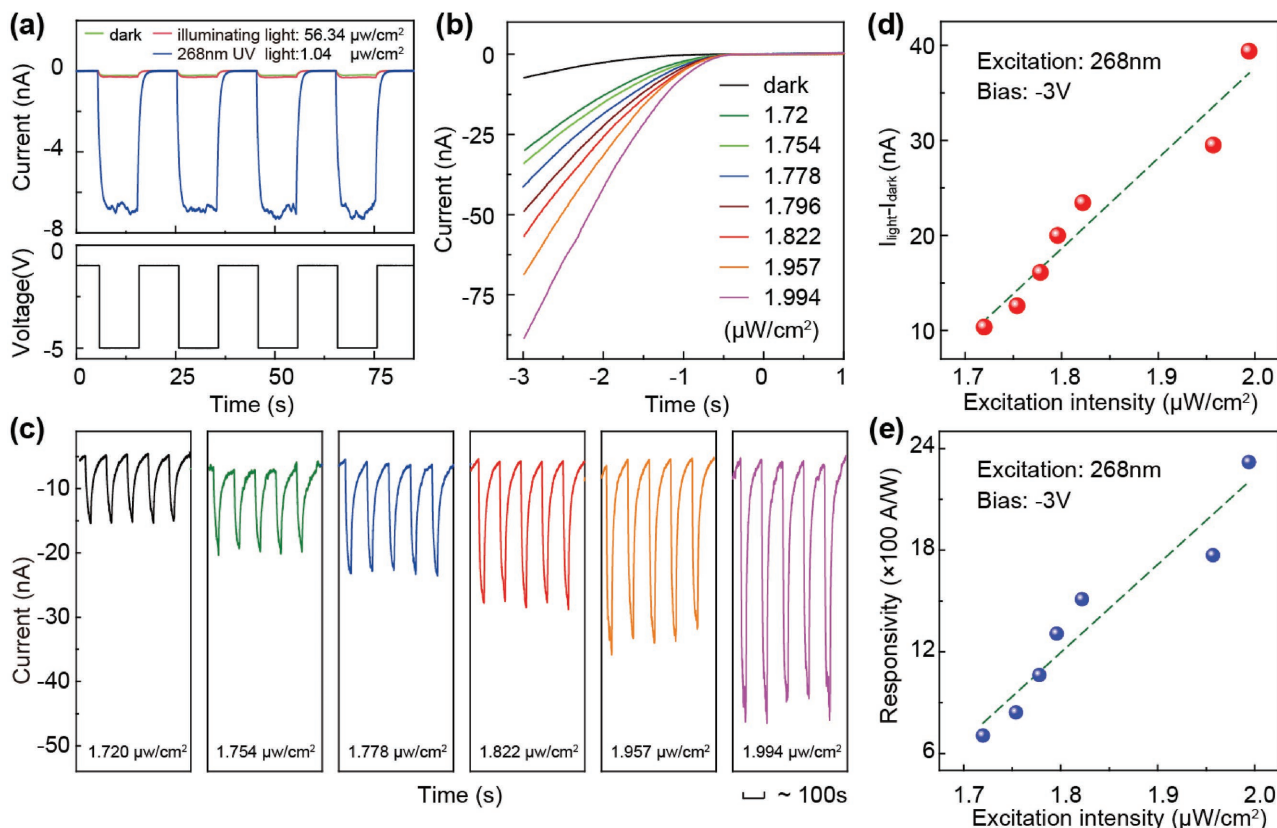


Figure 2. Optical properties of the solar-blinded microwire PD. a) Responses to 1.04 μW cm⁻² 268 nm UV light, 56.34 μW cm⁻² normal illuminating light and in dark environment with a rectangular wave stimuli, respectively. This shows a good wavelength selectivity. b) Reversed biased *I*-*V* curves under 268 nm UV light with different intensities. c) -1.5 V biased on-off *I*-*t* curves under 268 nm UV light with different intensities. d,e) Responsivity of the device. Solar blind illumination intensity dependences of photocurrent ($I_{light} - I_{dark}$) and photoresponsivity *R* measured at -3 V.

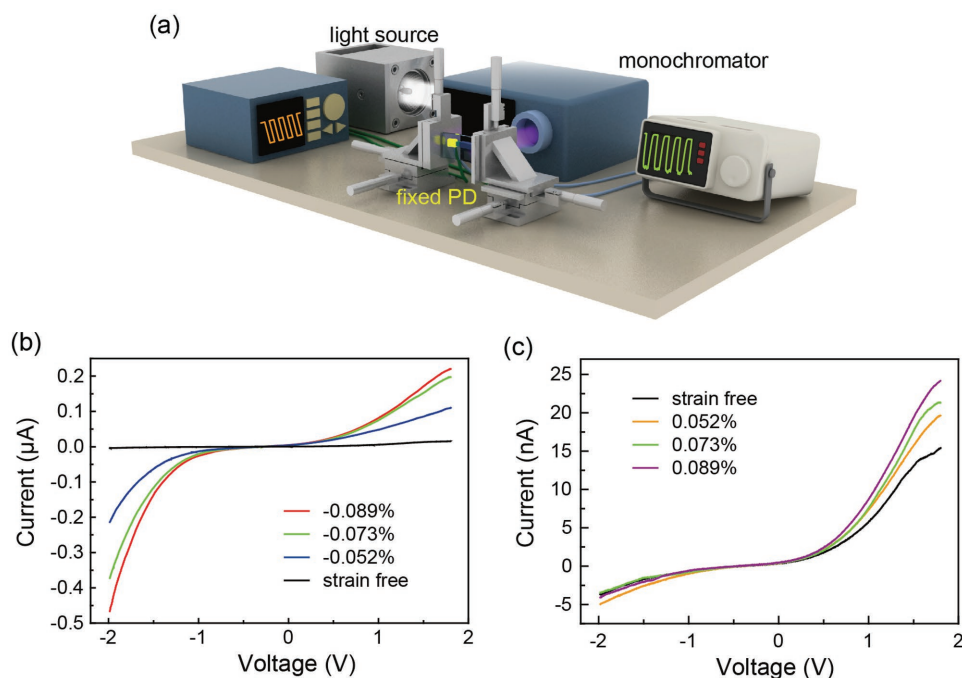


Figure 3. The piezoelectric effect on solar-blinded microwire PD. a) Experimental setup to measure the optical responses and modulation by external strains. b,c) I - V characteristics of the same PD under compressive b) and tensile strains c), obtained by applying a triangular wave across the device swiping from -2 to $+2$ V, showing an piezoelectric modulation performance.

compressive strains applied on the device, an asymmetrical phenomenon was observed. The enhanced effect was more obvious under reversely biased conditions than under forward biased conditions (Figure 3b). While when tensile strains applied on the same device, it shows an opposite result: the enhanced effect was more obvious under forward biased conditions with almost no change under reversely biased conditions (Figure 3c). The compressive strain performed a more effective regulating impact. The asymmetrical results confirmed the piezoelectric effect modulation in this ZnO core-Ga₂O₃ shell microwire solar-blinded PD device. Then we could systematically study the piezo-phototronic effect in this solar-blinded PD device.

Figure 4a,b is strain enhanced detections under $1.3 \mu\text{W cm}^{-2}$ 268 nm UV light. The dashed line and solid line in the same color represent responses in the dark condition and under 268 nm UV light illumination, respectively. The current response was enhanced about three times under -0.042% strain. To deeply understand the working mechanism of the strain modulation process in the PD device, we proposed a theoretical model to analyze the obtained results based on previous works.^[16a,21] Figure 4c shows the schematic of carrier transport under reversely biased voltage. Figure 4d further demonstrates carrier generation under UV light illumination, which happens both in the Ga₂O₃ shell and ZnO core. The bandgap of Ga₂O₃ is 4.9 eV, the bandgap of ZnO is 3.37 eV, and the deep UV light could transmit into the ZnO core area. In Figure 4e,f, the color indicates that the piezopotential distribution in the ZnO core under compressive and tensile strains with red represents positive potential and blue represents negative potential. When compressive strain was applied on the device, the

piezopotential introduced strengthened the electron transport in the ZnO core, thus the photocurrent was obviously enhanced. However, when tensile strain was applied, there was not obvious change in photocurrent as compressive strain did. This is because the opposite piezopotential was introduced, and there is no enhanced effect. Beside this dominated modulation mechanism, the piezo-phototronic effect also regulates the photogenerated carrier at the junction area (Figure S7, Supporting Information) which makes the photocurrent remain almost unchanged under tensile strains. It is a multiprocess when the piezo-phototronic effect tunes the photodetection in the ZnO-Ga₂O₃ core-shell structure.

3. Conclusion

In summary, we developed a strain modulated solar-blinded avalanche photodetector based on ZnO-Ga₂O₃ core-shell heterojunction microwire. This PD is highly sensitive to deep UV light centered at 261 nm. It demonstrated ultrahigh sensitivity and spectral selectivity, which could respond to rare weak deep UV light with almost no response to visible light. Moreover, the detection could be enhanced by applying certain static strains on the device through the piezo-phototronic effect. The current response could be enhanced about three times under -0.042% strain. The strain induced piezopotential modulates carrier transport mainly in the ZnO core. The photoresponse of this PD was enhanced by this effect, and thus made it a more perspective PD in human-machine interaction area,^[22] such as health monitoring, smart systems,^[23] and security communication.

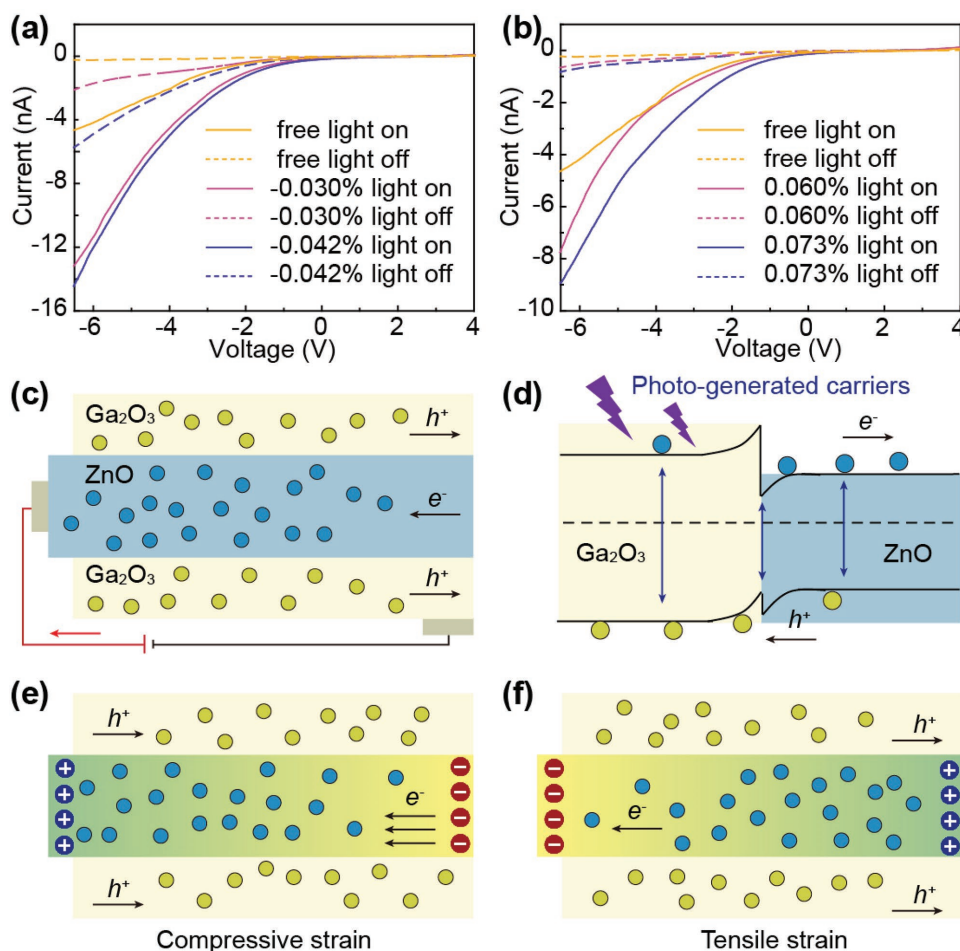


Figure 4. The piezo-phototronic effect on the solar-blinded microwire PD. a,b) I - V response to $1.3 \mu\text{W cm}^{-2}$ 268 nm UV light under compressive strains and tensile strains respectively. c,d) Schematic diagram exhibiting the energy band structure, electron-hole pair separation, and transfer in the ZnO-Ga₂O₃ heterostructure under light illumination of solar-blinded UV light centered at 268 nm. e,f) The proposed model of the device under strains, that is, electron transport is modulated in ZnO core by the piezopotential and the color indicates the piezopotential distribution in the ZnO core under compressive and tensile strains. The other coexisting process under the piezo-phototronic effect is listed in Supporting Information.

4. Experimental Section

Growth of ZnO-Ga₂O₃ Core-Shell Microwires: The ZnO-Ga₂O₃ core-shell microwires were synthesized via a simple one-step CVD method, a mixture of ZnO, Ga₂O₃, and graphite powders were used as the reactant source material with a weight ratio of 1:0.1:1. A 100 nm thick ZnO seed layer was deposited via a radio frequency magnetron sputtering method on a silicon substrate. The substrate was then deposited on the source material. The furnace was heated to 1200 °C at a rate of 25 °C min⁻¹ under a constant flow of Ar (160 standard cubic centimeters per minute) as the protecting gas. Then maintained at 1200 °C for 40 min and cooled down to room temperature naturally. Finally the ZnO-Ga₂O₃ microwires were synthesized on the substrate.

Device Construction: A single ZnO-Ga₂O₃ core-shell microwire was selected and transferred to the PET substrate. Then silver pastes were used to serve as the electrodes for both ends and the shell of microwire. The diameters of as grown microwires are different. The average diameter of the microwires is 5–10 μm, however it could be as small as 200 nm. The lengths of microwires for different devices are not the same. The length range is 100–200 μm, so the length difference could be tens of micrometers. These differences may lead to response differences among different devices (e.g., devices in Figures 3 and 4).

Test Platform: The light with a certain wavelength was gained with a laser-driven light source (white light) and a monochromator. The light intensity was regulated by adjusting the distance between the light exit of monochromator and the 3D stage on which the device was fixed. The light intensity was measured by Thorlabs PM100D. When the device was under a stimuli from the signal generator, e.g., a rectangular wave, the connected electrometer could detect the current change of the device when there was light illumination, thus the photocurrent was obtained.

Supporting Information

Supporting Information is available online from the Wiley Online Library or from the author.

Acknowledgements

M.C., B.Z., and G.H. contributed equally to this work. The authors are thankful for support from the “Thousand Talents” program of China for pioneering researchers and innovative teams and from the President Funding of the Chinese Academy of Sciences, National Natural Science

Foundation of China (Nos. 51432005, 5151101243, 51561145021, 61405040, 61505010, and 51502018), Beijing City Committee of Science and Technology (Z151100003315010).

Conflict of Interest

The authors declare no conflict of interest.

Keywords

deep UV photodetectors, heterojunction microwires, piezo-phototronic effects, ZnO-Ga₂O₃

Received: November 2, 2017

Revised: January 1, 2018

Published online:

- [1] a) H. Kind, H. Yan, B. Messer, M. Law, P. Yang, *Adv. Mater.* **2002**, 14, 158; b) P. Peumans, A. Yakimov, S. R. Forrest, *J. Appl. Phys.* **2003**, 93, 3693.
- [2] a) M. Peng, Z. Li, C. Liu, Q. Zheng, X. Shi, M. Song, Y. Zhang, S. Du, J. Zhai, Z. L. Wang, *ACS Nano* **2015**, 9, 3143; b) X. Wang, M. Que, M. Chen, X. Han, X. Li, C. Pan, Z. L. Wang, *Adv. Mater.* **2017**, 29, 1605817.
- [3] Y. Kishimoto, J. Abe, *J. Am. Chem. Soc.* **2009**, 131, 4227.
- [4] a) Z. Wang, R. Yu, X. Wang, W. Wu, Z. L. Wang, *Adv. Mater.* **2016**, 28, 6880; b) F. Xue, L. Chen, J. Chen, J. Liu, L. Wang, M. Chen, Y. Pang, X. Yang, G. Gao, J. Zhai, *Adv. Mater.* **2016**, 28, 3391; c) W. Yang, S. Hullavarad, B. Nagaraj, I. Takeuchi, R. Sharma, T. Venkatesan, R. Vispute, H. Shen, *Appl. Phys. Lett.* **2003**, 82, 3424.
- [5] a) T. Oshima, T. Okuno, S. Fujita, *Jpn. J. Appl. Phys.* **2007**, 46, 7217; b) Y. Li, T. Tokizono, M. Liao, M. Zhong, Y. Koide, I. Yamada, J. J. Delaunay, *Adv. Funct. Mater.* **2010**, 20, 3972; c) W. Y. Kong, G. A. Wu, K. Y. Wang, T. F. Zhang, Y. F. Zou, D. D. Wang, L. B. Luo, *Adv. Mater.* **2016**, 28, 10725.
- [6] Q. Miaoling, Z. Ranran, W. Xiandi, Y. Zuqing, H. Guofeng, P. Caofeng, *J. Phys.: Condens. Matter* **2016**, 28, 433001.
- [7] a) M. Orita, H. Ohta, M. Hirano, H. Hosono, *Appl. Phys. Lett.* **2000**, 77, 4166; b) Z. Ji, J. Du, J. Fan, W. Wang, *Opt. Mater.* **2006**, 28, 415.
- [8] Z. L. Wang, W. Wu, *Natl. Sci. Rev.* **2014**, 1, 62.
- [9] a) B. Zhao, F. Wang, H. Chen, Y. Wang, M. Jiang, X. Fang, D. Zhao, *Nano Lett.* **2015**, 15, 3988; b) C. Jin, S. Park, H. Kim, C. Lee, *Sens. Actuators, B* **2012**, 161, 223.
- [10] Z. L. Wang, J. Song, *Science* **2006**, 312, 242.
- [11] M. Peng, Y. Liu, A. Yu, Y. Zhang, C. Liu, J. Liu, W. Wu, K. Zhang, X. Shi, J. Kou, *ACS Nano* **2015**, 10, 1572.
- [12] C. Pan, S. Niu, Y. Ding, L. Dong, R. Yu, Y. Liu, G. Zhu, Z. L. Wang, *Nano Lett.* **2012**, 12, 3302.
- [13] a) X. Han, W. Du, R. Yu, C. Pan, Z. L. Wang, *Adv. Mater.* **2015**, 27, 7963; b) X. Han, M. Chen, C. Pan, Z. L. Wang, *J. Mater. Chem.* **2016**, 4, 11341; c) Z. Wang, R. Yu, X. Wen, Y. Liu, C. Pan, W. Wu, Z. L. Wang, *ACS Nano* **2014**, 8, 12866.
- [14] a) C. Pan, M. Chen, R. Yu, Q. Yang, Y. Hu, Y. Zhang, Z. L. Wang, *Adv. Mater.* **2016**, 28, 1535; b) M. Chen, C. Pan, T. Zhang, X. Li, R. Liang, Z. Wang, *ACS Nano* **2016**, 10, 6074; c) X. Li, M. Chen, R. Yu, T. Zhang, D. Song, R. Liang, Q. Zhang, S. Cheng, L. Dong, A. Pan, *Adv. Mater.* **2015**, 27, 4447.
- [15] a) L. Zhu, L. Wang, C. Pan, L. Chen, F. Xue, B. Chen, L. Yang, L. Su, Z. L. Wang, *ACS Nano* **2017**, 11, 1894; b) W. Guo, C. Xu, G. Zhu, C. Pan, C. Lin, Z. L. Wang, *Nano Energy* **2012**, 1, 176.
- [16] a) Y. Liu, S. Niu, Q. Yang, B. D. Klein, Y. S. Zhou, Z. L. Wang, *Adv. Mater.* **2014**, 26, 7209; b) W. Z. Wu, C. F. Pan, Y. Zhang, X. N. Wen, Z. L. Wang, *Nano Today* **2013**, 8, 619.
- [17] R. Yu, S. Niu, C. Pan, Z. L. Wang, *Nano Energy* **2015**, 14, 312.
- [18] X. Yu, X. Han, Z. Zhao, J. Zhang, W. Guo, C. Pan, A. Li, H. Liu, Z. Lin Wang, *Nano Energy* **2015**, 11, 19.
- [19] R. Yu, W. Wu, C. Pan, Z. Wang, Y. Ding, Z. L. Wang, *Adv. Mater.* **2015**, 27, 940.
- [20] B. Zhao, F. Wang, H. Chen, L. Zheng, L. Su, D. Zhao, X. Fang, *Adv. Funct. Mater.* **2017**, 27, 1700264.
- [21] a) F. Zhang, Y. Ding, Y. Zhang, X. Zhang, Z. L. Wang, *ACS Nano* **2012**, 6, 9229; b) F. Zhang, S. Niu, W. Guo, G. Zhu, Y. Liu, X. Zhang, Z. L. Wang, *ACS Nano* **2013**, 7, 4537.
- [22] P. Bartu, R. Koeppel, A. Neuling, S. Isikatanlar, S. Bauer, *Procedia Eng.* **2010**, 5, 295.
- [23] C. Xu, C. Pan, Y. Liu, Z. L. Wang, *Nano Energy* **2012**, 1, 259.